Structure and Properties of CeNiZn and CeAuZn

Wilfried Hermes[a], Ratikanta Mishra[a,b], Ute Ch. Rodewald[a], and Rainer Pöttgen[a]

[a] Institut für Anorganische und Analytische Chemie, Universität Münster, Corrensstraße 30, 48149 Münster, Germany
[b] Chemistry Division, Bhabha Atomic Research Centre Trombay, Mumbai-400 085, India

Reprint requests to R. Pöttgen. E-mail: pottgen@uni-muenster.de

Z. Naturforsch. **2008**, *63b,* 537 – 542; received January 10, 2008

Well crystallized samples of the intermetallic zinc compounds CeNiZn and CeAuZn were synthesized from the elements in sealed tantalum ampoules. They were investigated by X-ray diffraction on powders and single crystals. CeNiZn: ZrNiAl type, space group $P\bar{6}2m$, $Z = 3$, $a = 713.3(3)$, $c = 388.7(1)$ pm, $wR2 = 0.0422$ for 14 refined variables and 286 F^2 values; CeAuZn: TiNiSi type, space group *Pnma*, $Z = 4$, $a = 719.2(2)$, $b = 462.7(1)$, $c = 796.5(2)$ pm, $wR2 = 0.0403$ for 20 refined variables and 467 F^2 values. Magnetic susceptibility data reveal that CeNiZn is an intermediate-valent cerium compound with essentially tetravalent cerium. CeAuZn shows Curie-Weiss paramagnetism with an experimental magnetic moment of 2.51(1) μ_B per Ce atom and $\theta_P = -70(1)$ K. No magnetic ordering is observed down to 2.1 K.

Key words: Zinc, Intermetallics, Crystal Chemistry, Magnetism

Introduction

The equiatomic Ce*TX* compounds (*T* = late transition metal; *X* element of the 3rd, 4th, or 5th main group) have been intensively studied over the past 30 years with respect to their widely varying magnetic properties. Most of these compounds crystallize with the orthorhombic TiNiSi- [1] or ZrNiAl-type [2 – 4] structures. Variation of the valence electron concentration (VEC) through *T* and/or *X* substitution leads to different hybridization of the Ce 4*f* orbitals with the transition metal *d* states, leading to manifold magnetic behavior, *e. g.* antiferro- or ferromagnetism, intermediate cerium valence, Kondo-type behavior, superconductivity, or non-Fermi-liquid behavior.

In recent investigations we were able to show that further reduction of the VEC and thus variation of the magnetic properties is possible through substitution of the trivalent element *X* by magnesium or cadmium. To give an example, CePtIn is a dense Kondo compound without magnetic ordering down to 50 mK [5], while isotypic CePtMg shows long-range magnetic ordering at 3.6 K [6]. Upon going from CePdIn [7] to CePdMg [6] we observe an increase of the Néel temperature from 1.65 to 2.1 K.

In continuation of our systematic studies on Ce*T*Mg [6, 8, 9, and refs. therein] and Ce*T*Cd compounds [10, 11], we also investigated Ce*T*Zn intermetallics with the same electron count. So far, only X-ray powder diffraction data have been reported for CeCuZn [12, 13], CeAgZn [13], CeNiZn, and CePdZn [14]. The structure of TiNiSi-type CePtZn has recently been refined on the basis of single crystal data [15]. CePtZn shows trivalent cerium but no magnetic ordering down to 2 K. Herein we report on the structure and magnetic properties of the intermediate-valent system CeNiZn and the new compound CeAuZn.

Experimental Section

Synthesis

Starting materials for the preparation of the CeNiZn and CeAuZn samples were cerium ingots (Johnson Matthey), nickel wire (Johnson Matthey, ∅ 0.38 mm), a gold bar (Heraeus, rolled to gold foil), and zinc granules (Merck), all with stated purities better than 99.9 %. Pieces of the larger cerium ingot were first arc-melted [16] to a small button under an argon atmosphere. The argon was purified with molecular sieves, silica gel, and titanium sponge (900 K). Subsequently the cerium button, pieces of nickel wire (the gold foil) and pieces of the zinc granules (1 : 1 : 1 atomic ratio) were sealed in tantalum tubes under an argon pressure of *ca.* 700 mbar. The tubes were then placed in a water-cooled sample chamber of a high-frequency furnace (Hüttinger Elektronik, Freiburg, type TIG 1.5/300) under flowing argon [17] and was annealed at 1600 K for about five minutes followed

Table 1. Crystal data and structure refinement for CeNiZn and CeAuZn.

Empirical formula	CeNiZn	CeAuZn
Molar mass, g mol^{-1}	264.20	402.46
Space group; Z	$P\bar{6}2m$; 3	*Pnma*; 4
Structure type	ZrNiAl	TiNiSi
Pearson symbol	hP9	oP12
Unit cell dimensions, pm	$a = b = 713.3(3)$	$a = 719.2(2)$
(Guinier powder data)		$b = 462.7(1)$
	$c = 388.7(1)$	$c = 796.5(2)$
Cell volume, nm^3	0.1713	0.2651
Calculated density, g cm^{-3}	7.68	10.09
Crystal size, μm^3	$30 \times 30 \times 60$	$10 \times 40 \times 40$
Detector distance, mm	–	80
Exposure time, min	–	13
ω range; increment, deg	–	0 – 180; 1.0
Integr. param. A; B; EMS	–	13.5; 3.5; 0.014
Radiation	AgK_α	MoK_α
Wave length λ, pm	56.086	71.073
Transm. ratio (max/min)	1.57	2.60
Absorption coefficient, mm^{-1}	19.8	80.7
F(000), e	348	668
θ range, deg	2 – 26	3 – 31
hkl range	± 11;	± 10;
	± 11;	± 6;
	$-6 / +3$	± 11
Total no. reflections	2179	2818
Independent reflections	286	467
	($R_{\text{int}} = 0.069$)	($R_{\text{int}} = 0.061$)
Reflections with $I \geq 2\sigma(I)$	271	336
	($R_\sigma = 0.033$)	($R_\sigma = 0.066$)
Data / ref. parameters	286 / 14	467 / 20
Goodness-of-fit on F^2	1.055	0.787
Final R indices [$I \geq 2\sigma(I)$]	$R1 = 0.021$	$R1 = 0.023$
	$wR2 = 0.041$	$wR2 = 0.039$
Final R indices (all data)	$R1 = 0.024$	$R1 = 0.041$
	$wR2 = 0.042$	$wR2 = 0.040$
Extinction coefficient	0.056(3)	0.0028(1)
Flack parameter	0.2(3)	–
Largest diff. peak and hole, e Å^{-3}	1.29 / −1.23	1.85 / −2.25

by slow cooling to 920 K. Finally the samples were kept at that temperature for another 6 h, followed by quenching. The temperature was controlled through a Sensor Therm Methis MS09 pyrometer with an accuracy of ±30 K. The samples could easily be separated from the crucible material. No reaction with the container was observed. CeNiZn and CeAuZn are stable in air over weeks. Single crystals exhibit metallic lustre while the ground powder is grey.

X-Ray powder data

The CeNiZn and CeAuZn samples were studied by Guinier powder patterns using Cu$K_{\alpha 1}$ radiation and α-quartz (a = 491.30, c = 540.46 pm) as an internal standard. The Guinier camera was equipped with an imaging plate system (Fujifilm, BAS-1800). The lattice parameters (Table 1) were refined by least-squares calculations. The correct indexing was ensured through intensity calculations [18], taking the atomic sites obtained from the structure refinements. For CeNiZn our lattice parameters are in good agreement with those reported by Iandelli (a = 714.1(1), c = 388.8(1) pm) [14].

Single crystal X-ray diffraction

Irregularly shaped crystals of CeNiZn and CeAuZn were selected from the crushed annealed samples. These crystals were glued onto small quartz fibres using bees wax and first checked by Laue photographs on a Buerger camera, equipped with the same Fujifilm, BAS-1800 imaging plate technique. Intensity data of the CeNiZn crystal were collected at r. t. on a four-circle diffractometer (CAD4) with graphite-monochromatized AgK_α radiation and a scintillation counter with pulse-height discrimination. Scans were taken in the $\omega/2\theta$ mode. An empirical absorption correction was applied on the basis of ψ scan data, accompanied by a spherical absorption correction. The CeAuZn crystal was measured on a Stoe IPDS II diffractometer (graphite-monochromatized MoK_α radiation; oscillation mode), and a numerical absorption correction was applied to the data set. Relevant crystallographic data for the data collections and structure refinements are listed in Table 1.

Scanning electron microscopy

The single crystals investigated on the diffractometer were analyzed using a LEICA 420 I scanning electron microscope with CeO_2, Ni, Au, and Zn as standards. No impurity elements heavier than sodium (detectability level of the instrument) were observed. The semiquantitatively obtained compositions determined by EDX were close to the ideal equiatomic composition.

Property measurements

The CeNiZn and CeAuZn samples were packed in kapton foil and attached to the sample-holder rod of a VSM for measuring the magnetic properties in a Quantum Design Physical-Property-Measurement System in the temperature range 3 – 305 K with magnetic flux densities up to 80 kOe. For heat capacity (C_p) measurements (T = 2.1 – 50 K) the CeAuZn sample was glued to the platform of a pre-calibrated heat capacity puck using Apiezon N grease.

Structure refinements

Careful analyses of the diffractometer data sets revealed high Laue symmetry for both crystals. The data sets were compatible with space groups $P\bar{6}2m$ for CeNiZn and *Pnma* for CeAuZn. The isotypism with the ZrNiAl and TiNiSi structure types was already evident from the powder diffraction data. The atomic coordinates of CePtMg [6] and CePtZn

Table 2. Atomic coordinates and anisotropic displacement parameters (pm^2) for CeNiZn and CeAuZn. U_{eq} is defined as one third of the trace of the orthogonalized U_{ij} tensor. The anisotropic displacement factor exponent takes the form $-2\pi^2[(ha^*)^2U_{11} + \ldots + 2khka^*b^*U_{12}]$. $U_{23} = 0$.

Atom	Wyckoff position	x	y	z	U_{11}	U_{22}	U_{33}	U_{12}	U_{13}	U_{eq}
CeNiZn:										
Ce	3*f*	0.41576(7)	0	0	101(2)	99(3)	88(2)	50(1)	0	96(2)
Ni1	1*a*	0	0	0	139(6)	U_{11}	108(12)	70(3)	0	129(5)
Ni2	2*d*	2/3	1/3	1/2	149(5)	U_{11}	127(9)	75(3)	0	142(4)
Zn	3*g*	0.76498(18)	0	1/2	122(4)	126(5)	125(6)	63(3)	0	124(3)
CeAuZn:										
Ce	4*c*	0.00756(11)	1/4	0.71153(9)	85(3)	103(4)	94(3)	0	−2(3)	94(2)
Au	4*c*	0.28311(7)	1/4	0.41055(8)	122(2)	76(3)	79(2)	0	11(3)	92(2)
Zn	4*c*	0.69044(18)	1/4	0.4199(2)	143(7)	39(8)	37(7)	0	−5(6)	73(3)

Table 3. Interatomic distances (pm) as calculated with the powder lattice parameters of CeNiZn and CeAuZn. Standard deviations are all equal or less than 0.2 pm. All distances of the first coordination sphere are listed.

CeNiZn				CeAuZn			
Ce:	4	Ni2	289.5	Ce:	1	Au	311.0
	1	Ni1	296.6		2	Au	318.3
	2	Zn	315.9		2	Zn	318.3
	4	Zn	322.7		1	Zn	321.7
	4	Ce	371.5		1	Zn	325.6
	2	Ce	388.7		2	Au	326.6
					2	Zn	334.1
					1	Au	341.6
					2	Ce	364.8
					2	Ce	408.9
Ni1:	6	Zn	256.7	Au:	2	Zn	268.6
	3	Ce	296.6		1	Zn	271.5
Ni2:	3	Zn	279.5		1	Zn	293.0
	6	Ce	289.5		1	Ce	311.0
					2	Ce	318.3
					2	Ce	326.6
					1	Ce	341.6
Zn:	2	Ni1	256.7	Zn:	2	Au	268.6
	2	Ni2	279.5		1	Au	271.5
	2	Zn	290.4		1	Au	293.0
	2	Ce	315.9		2	Ce	318.3
	4	Ce	322.7		1	Ce	321.7
					1	Ce	325.6
					2	Ce	334.1

[15] were taken as starting values, and both structures were refined with anisotropic displacement parameters for all atoms with SHELXL-97 (full-matrix least-squares methods on F_o^2) [19]. Refinement of the correct absolute structure for CeNiZn was ensured through calculation of the Flack parameter [20, 21]. The occupancy parameters were refined in seperate series of least-squares cycles as a check for deviations from the equiatomic composition. All sites were fully occupied within two standard deviations, and in the final refinement cycles the ideal occupancies were assumed again. The refinements converged to the residuals listed in Table 1. Final difference Fourier syntheses revealed no significant residual peaks. The atomic parameters and interatomic distances are listed in Tables 2 and 3.

Further details of the crystal structure investigations may be obtained from Fachinformationszentrum Karlsruhe, 76344 Eggenstein-Leopoldshafen, Germany (fax: +49-7247-808-666; e-mail: crysdata@fiz-karlsruhe.de, http://www.fiz-informationsdienste.de/en/DB/icsd/depot_anforderung.html) on quoting the deposition numbers CSD-418711 (CeNiZn) and CSD-418712 (CeAuZn).

Results and Discussion

Crystal chemistry

The equiatomic cerium intermetallics CeNiZn and CeAuZn have been synthesized and their structures have been refined on the basis of single crystal X-ray diffractometer data. So far, only X-ray powder diffraction data have been reported for CeNiZn [14]. The nickel compound adopts the hexagonal ZrNiAl-type [2 – 4] structure, and CeAuZn crystallizes with the TiNiSi type [1]. The course of the cell volumes in the *RE*NiZn series (*RE* = rare earth elements) [14] reveals a large anomaly for the cerium compound. The cell volume of CeNiZn is even smaller than that of PrNiZn, a clear sign for at least partially tetravalent cerium (see the magnetic data discussed below). The structural chemistry of TiNiSi- and ZrNiAl-related intermetallic compounds have repeatedly been discussed [22 – 28]. For details and drawings we refer to the literature. Herein we focus only on some structural peculiarities of CeNiZn and CeAuZn.

The shortest interatomic distances in the CeNiZn and CeAuZn structures occur for Ni–Zn (257 – 280 pm) and Au–Zn (269 – 293 pm). They are both slightly longer than the sums of the covalent radii (Σr_{cov} = 240 pm for Ni + Zn and 259 pm for Au + Zn)

[29]. Similar to the Ce*T*Mg compounds [6], these transition metal-zinc contacts have most probably moderate bonding character. The transition metal and zinc atoms in CeNiZn and CeAuZn build up three-dimensional [NiZn] and [AuZn] networks which leave channels for the cerium atoms. The latter bind to these networks *via* Ce-*T* contacts, *i. e.* 290 – 297 pm for Ce–Ni and 311 pm for Ce–Au. However, also these distances are slightly longer than the sums of the covalent radii (Σr_{cov} = 280 pm for Ce + Ni and 299 pm for Ce + Au) [29].

An interesting point is the course of the Ce–Ce distances (372 – 389 pm in CeNiZn and 365 – 409 pm in CeAuZn). All of these Ce–Ce distances are longer than the Hill limit (340 pm) for *f* electron localization [30]. The shorter Ce–Ce distance in CeAuZn compares well with the Ce–Ce distance of 365 pm in *fcc* cerium [31]. In contrast to CePtZn (*d*(Ce–Ce) = 366 and 382 pm) [15], the Ce–Ce distances in CeAuZn (409 pm) are significantly longer. This is a direct consequence of the course of the lattice parameters, *i. e.* *a* = 719.2, *b* = 462.7, *c* = 796.5 pm for CeAuZn while *a* = 706.9, *b* = 435.1, *c* = 809.7 pm for CePtZn. This results in different tilts of the T_2Zn_2 rhombs within the [*T*Zn] networks, leading to a slightly different bonding pattern. Thus, CeNiZn and CeAuZn lie in different structural branches of the family of *anti*-$PbCl_2$-related compounds. All these compounds can be grouped on the basis of the axial ratios *a*/*c* and (*a*+*c*)/*b* [32].

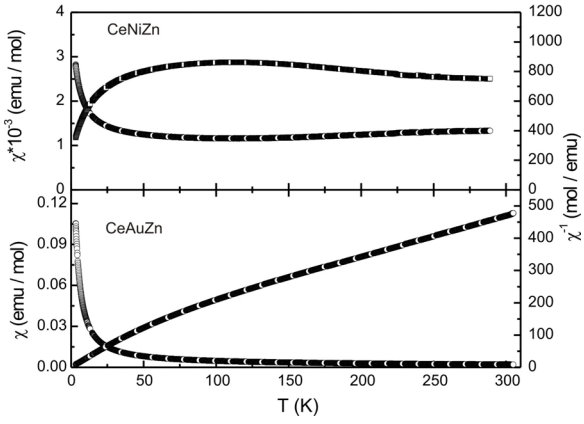

Fig. 1. The magnetic and inverse magnetic susceptibility of CeNiZn and CeAuZn measured at a magnetic flux density of 10 kOe.

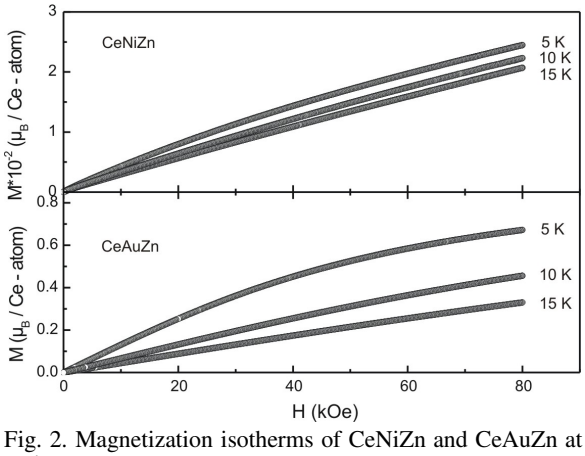

Fig. 2. Magnetization isotherms of CeNiZn and CeAuZn at various temperatures.

Magnetic properties

The temperature dependence of the magnetic and the inverse magnetic susceptibility of CeNiZn and CeAuZn are displayed in Fig. 1. CeNiZn shows a small and only weakly temperature-dependent susceptibility which is typical for an intermediate-valent cerium compound. The upturn of the susceptibility at low temperatures is due to defects and impurities. This behavior is almost similar to Ce_2Ni_2Mg [33] and CeRhIn [34]. A fit of the susceptibility in the temperature region 5 – 100 K according to a modified Curie-Weiss expression revealed $\chi_o = 1.05 \times 10^{-2}$ emu mol^{-1}, μ_{eff} = 0.29(1) μ_B per Ce atom and $\theta_P = -2.80(2)$ K. Since the experimental magnetic moment is much smaller than the free ion value of 2.54 μ_B for Ce^{3+}, we can assume essentially tetravalent cerium in CeNiZn (C = 0.0106 emu mol^{-1} K^{-1}, *i. e.* $\sim$ 1.3 % Ce^{3+}), in good agreement with the course of the cell volumes in the *RE*NiZn series (*vide supra*) [14]. The magnetization isotherms (Fig. 2) at 5, 10, and 15 K are almost linear with extremely small magnetization values at the highest obtainable field of 80 kOe.

CeAuZn shows Curie-Weiss behavior (Fig. 1). Fitting of the experimental data in the temperature region 100 – 300 K revealed an effective magnetic moment of μ_{eff} = 2.51(1) μ_B per Ce atom and $\theta_P = -70(1)$ K, indicating pure trivalent cerium in CeAuZn. The deviations of $1/\chi$ *vs.* T at low temperatures is most likely due to splitting of the J = 5/2 ground state of Ce^{3+} and the beginning short-range magnetic fluctuations, as it was frequently observed in related cerium intermetallics, *e. g.* in CeAuGe [35] or $CeRhSn_2$ [36].

The magnetization of CeAuZn (Fig. 2) varies in an almost linear fashion at temperatures of 10 and 15 K as expected for a paramagnetic material. At 5 K the

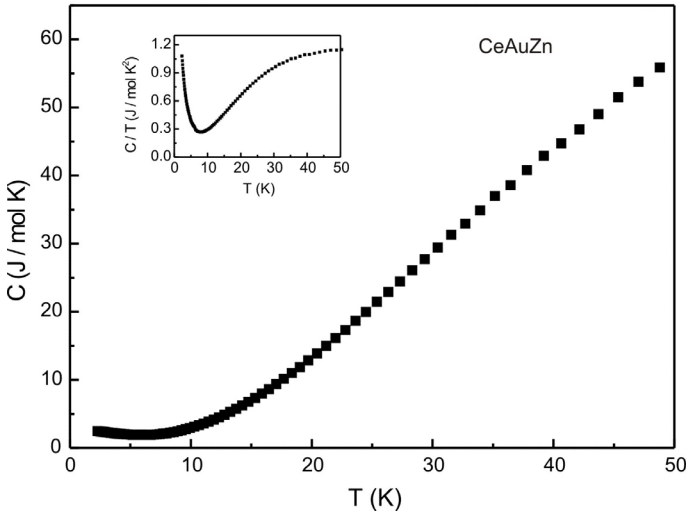

Fig. 3. Temperature dependence of the specific heat of CeAuZn (as *C*/*T vs*. *T* plot in the inset) measured in zero magnetic field.

curvature becomes more pronounced and the magnetization at 5 K and 80 kOe is 0.67 μ_B per Ce atom, which is *ca.* 33 % of the maximum possible value of $g_J \times J = 2.14\ \mu_B$ for Ce^{3+}. Such reduced magnetization values often occur in intermetallic cerium compounds and can be attributed to crystal field splitting of the J = 5/2 ground state of Ce^{3+}. The magnetic and specific heat data (Fig. 3) give no hint for magnetic ordering in CeAuZn down to 2.1 K.

Acknowledgements

We thank Dipl.-Chem. F. M. Schappacher for the work at the scanning electron microscope. This work was supported by the Deutsche Forschungsgemeinschaft. R. M. is indebted to the Alexander-von-Humboldt Foundation for a research fellowship. W. H. is indebted to the Stiftung Stipendienfonds des Fonds der Chemischen Industrie and to the NRW Graduate School of Chemistry for supporting the Ph. D. thesis.

[1] C. B. Shoemaker, D. P. Shoemaker, *Acta Crystallogr.* **1965**, *18*, 900.
[2] P. I. Krypyakevich, V. Ya. Markiv, E. V. Melnyk, *Dopov. Akad. Nauk. Ukr. RSR*, *Ser. A*, **1967**, 750.
[3] A. E. Dwight, M. H. Mueller, R. A. Conner, Jr., J. W. Downey, H. Knott, *Trans. Met. Soc. AIME* **1968**, *242*, 2075.
[4] M. F. Zumdick, R.-D. Hoffmann, R. Pöttgen, *Z. Naturforsch*. **1999**, *54b*, 45.
[5] H. Fujii, Y. Uwatoko, M. Akayama, K. Satoh, Y. Maeno, T. Fujita, J. Sakurai, H. Kamimura, T. Okamoto, *Jpn. J. Appl. Phys*. **1987**, *26*, 549.
[6] B. J. Gibson, A. Das, R. K. Kremer, R.-D. Hoffmann, R. Pöttgen, *J. Phys.: Condens. Matter* **2002**, *14*, 5173.
[7] E. Brück, M. van Sprang, J. C. P. Klaasse, F. R. de Boer, *J. Appl. Phys*. **1988**, *63*, 3417.
[8] D. Johrendt, G. Kotzyba, H. Trill, B. D. Mosel, H. Eckert, Th. Fickenscher, R. Pöttgen, *J. Solid State Chem.* **2002**, *164*, 201.
[9] U. Ch. Rodewald, B. Chevalier, R. Pöttgen, *J. Solid State Chem*. **2007**, *180*, 1720.
[10] R. Mishra, R. Pöttgen, R.-D. Hoffmann, D. Kaczorowski, H. Piotrowski, P. Mayer, C. Rosenhahn, B. D. Mosel, *Z. Anorg. Allg. Chem*. **2001**, *627*, 1283.
[11] Th. Fickenscher, R.-D. Hoffmann, R. Mishra, R. Pöttgen, *Z. Naturforsch*. **2002**, *57b*, 275.
[12] P. Morin, D. Gignoux, J. Voiron, A. P. Murani, *Physica B* **1992**, *180&181*, 173.
[13] M. L. Fornasini, A. Iandelli, F. Merlo, M. Pani, *Intermetallics* **2000**, *8*, 239.
[14] A. Iandelli, *J. Alloys Compd*. **1992**, *182*, 87.
[15] R. Mishra, W. Hermes, R. Pöttgen, *Z. Naturforsch*. **2007**, *62b*, 1581.
[16] R. Pöttgen, Th. Gulden, A. Simon, *GIT Labor Fachzeitschrift* **1999**, *43*, 133.
[17] D. Kußmann, R.-D. Hoffmann, R. Pöttgen, *Z. Anorg. Allg. Chem*. **1998**, *624*, 1727.
[18] K. Yvon, W. Jeitschko, E. Parthé, *J. Appl. Crystallogr.* **1977**, *10*, 73.
[19] G. M. Sheldrick, SHELXL-97, Program for Crystal Structure Refinement, University of Göttingen, Göttingen (Germany) **1997**.
[20] H. D. Flack, G. Bernadinelli, *Acta Crystallogr*. **1999**, *A55*, 908.
[21] H. D. Flack, G. Bernadinelli, *J. Appl. Crystallogr.* **2000**, *33*, 1143.

[22] G. Nuspl, K. Polborn, J. Evers, G. A. Landrum, R. Hoffmann, *Inorg. Chem*. **1996**, *35*, 6922.
[23] G. A. Landrum, R. Hoffmann, J. Evers, H. Boysen, *Inorg. Chem*. **1998**, *37*, 5754.
[24] R.-D. Hoffmann, R. Pöttgen, *Z. Kristallogr*. **2001**, *216*, 127.
[25] M. D. Bojin, R. Hoffmann, *Helv. Chim. Acta* **2003**, *86*, 1653.
[26] M. D. Bojin, R. Hoffmann, *Helv. Chim. Acta* **2003**, *86*, 1683.
[27] E. Parthé, L. Gelato, B. Chabot, M. Penzo, K. Cenzual, R. Gladyshevskii, *TYPIX–Standardized Data and Crystal Chemical Characterization of Inorganic Structure Types, Gmelin Handbook of Inorganic and Organometallic Chemistry*, (8th edition), Springer, Berlin **1993**.
[28] M. F. Zumdick, R. Pöttgen, *Z. Kristallogr*. **1999**, *214*, 90.
[29] J. Emsley, The Elements, Oxford University Press, Oxford **1999**.
[30] H. H. Hill in *Plutonium and other Actinides*, *Nuclear Materials Series, AIME*, (Ed.: W. N. Mines) **1970**, vol. *17*, pp. 2.
[31] J. Donohue, The Structures of the Elements, Wiley, New York **1974**.
[32] W. Jeitschko, R. O. Altmeyer, *Z. Naturforsch*. **1990**, *45b*, 947.
[33] C. Geibel, U. Klinger, M. Weiden, B. Buschinger, F. Steglich, *Physica B* **1997**, *237-238*, 202.
[34] D. T. Adroja, S. K. Malik, B. D. Padalia, R. Vijayaraghavan, *Phys. Rev. B* **1999**, *39*, 4831.
[35] R. Pöttgen, H. Borrmann, R. K. Kremer, *J. Magn. Magn. Mater*. **1996**, *152*, 196.
[36] D. Niepmann, R. Pöttgen, B. Künnen, G. Kotzyba, C. Rosenhahn, B. D. Mosel, *Chem. Mater*. **1999**, *11*, 1597.